THE JOURNAL OF PHYSICAL CHEMISTRY B

Article

Encapsulation of Small Ionic Molecules within #-Cyclodextrins

Javier Rodriguez, and M. Dolores Elola

J. Phys. Chem. B, **2009**, 113 (5), 1423-1428 • DOI: 10.1021/jp808947m • Publication Date (Web): 14 January 2009

Encapsulation of Small Ionic Molecules within α-Cyclodextrins

Javier Rodriguez*,† and M. Dolores Elola*

Departamento de Física de la Materia Condensada, Comisión Nacional de Energía Atómica, Av. General Paz 1499, 1650 San Martín, Prov. de Buenos Aires, Argentina

Received: October 9, 2008; Revised Manuscript Received: December 1, 2008

Results from molecular dynamics experiments pertaining to the encapsulation of ClO_4^- within the hydrophobic cavity of an aqueous α-cyclodextrin (α-CD) are presented. Using a biased sampling procedure, we constructed the Gibbs free energy profile associated with the complexation process. The profile presents a global minimum at the vicinity of the primary hydroxyl groups, where the ion remains tightly coordinated to four water molecules via hydrogen bonds. Our estimate for the global free energy of encapsulation yields $\Delta G_{enc} \sim -2.5\ k_BT$. The decomposition of the average forces acting on the trapped ion reveals that the encapsulation is controlled by Coulomb interactions between the ion and OH groups in the CD, with a much smaller contribution from the solvent molecules. Changes in the previous results, arising from the partial methylation of the host CD and modifications in the charge distribution of the guest molecule are also discussed. The global picture that emerges from our results suggests that the stability of the ClO_4^- encapsulation involves not only the individual ion but also its first solvation shell.

I. Introduction

One of the most distinctive characteristics associated with the behavior of cyclodextrins (CD) in solution is their ability to act as efficient complexation agents of a large variety of solute species.[1] This feature is commonly ascribed to their overall molecular geometry, normally portrayed in terms of a quasi-cylindrical cavity, 6−7 Å in height and 5−8 Å in diameter, surrounded by a number of glucopyranose units intermediate between 6 and 8.[2,3]

A large body of previous studies has demonstrated that the prevailing interactions at the inner and outer surfaces of CD cavities differ at a qualitative level.[1] The hydroxyl groups, located at the top and bottom rims of the CD, confer the outer surface a hydrophilic character. In contrast, the inner cavities represent environments with clear hydrophobic characteristics; the latter represent key elements that, in turn, would explain the high stability of inclusion complexes involving organic probes in aqueous solutions.

Complementary to these observations, it is also well documented that simple inorganic ions, such as alkali halides, SCN^- and ClO_4^-, can be encapsulated within CD cavities as well.[4,5] Information from spectrophotometric,[5,6] NMR,[7,8] X-ray,[9] calorimetric,[10,11] potentiometric[12,13] and conductance[4] experiments have revealed selective associations of many ionic species. Concerning the specific case of the encapsulation of simple anionic species in small α-cyclodextrins (six glucose units), there seems to be general consensus establishing that ClO_4^- exhibits one of the largest binding constants.[4,5] For cationic species, the complexation information always appears as complementary to that of the anions and is much less conclusive. In fact, there is not clear agreement about the influence of the identity of the counterion on the encapsulation constant.[7,13,14] From a microscopic perspective, the global picture that emerges from the available experimental information would suggest that the stability of CD-ion moieties would be the result of the complex interplay involving not only the usual Lennard-Jones and Coulomb-type interactions but also short-ranged forces that would affect the packing within the central cavities.[1,11] As such, and despite its apparent simplicity, many aspects related to the actual sources for the ionic stabilization and the microscopic characteristics of the encapsulation mechanisms remain poorly understood.

Given the previous description, the purpose of the present paper aims at the elucidation of microscopic characteristics associated to ionic encapsulation within CD using molecular dynamics techniques. In the last decade, this approach has been successfully implemented to analyze solvation of a large variety of relatively simple host-CD partners in vacuo and solution.[15] Recently, with the advent of more powerful computational resources and more sophisticated simulation tools,[16−29] it also became feasible to obtain thermodynamic information pertaining to the CD encapsulation of guests with much more complex molecular geometries, such as cholesterol or rotaxane in solution.[30,31] Within a similar spirit, in the present study, we present results from full atomistic, molecular dynamics simulations involving the complexation of ClO_4^- within an aqueous α-CD. To clearly identify the characteristics of the ionic encapsulation, we also performed additional runs analyzing the encapsulation of a cationic and a neutral molecule with similar geometry to that of the ClO_4^-.

The organization of the paper is as follows: In section III we present details of the systems and the methodology that we implemented to run the simulations. Section IV includes the results of our simulation experiments. The main conclusions of the paper are summarized in section IV.

II. Systems Studied and Simulation Details

The systems under investigation were composed of a single α-CD and a guest solute mimicking a ClO_4^- molecule, immersed in a cubic box containing $N_w = 2640$ water molecules. The dynamical trajectories corresponded to *NPT* simulation runs. Langevin dynamics were implemented to maintain the temperature and the external pressure close to $T = 298$ K and 1 bar,

* Corresponding author. E-mail: DoloresElola@gmail.com.
† E-mail: javier@speedy.cnea.gov.ar.

10.1021/jp808947m CCC: $40.75
Published on Web 01/14/2009

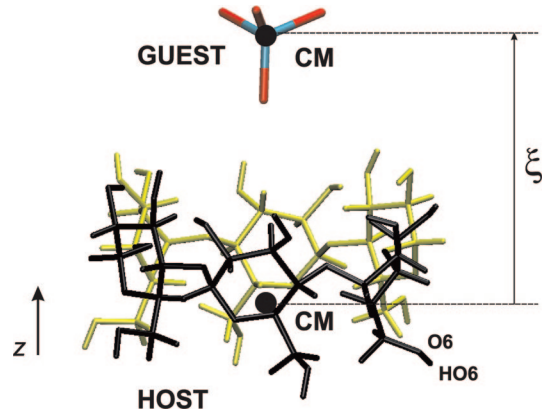

Figure 1. Initial configuration of the host−guest complex.

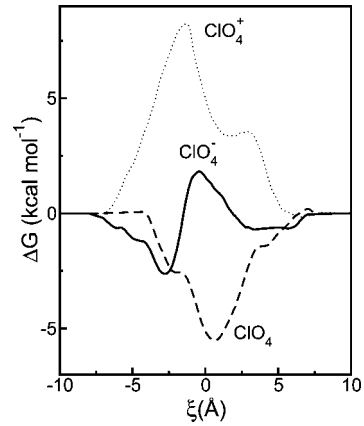

Figure 2. Gibbs free energy profiles for the inclusion of ClO_4-like molecules within an α-CD.

respectively. At these thermodynamic conditions, the length of the simulation box fluctuates around $L = 43$ Å. The dynamics were generated using the NAMD package,[32] with a force field corresponding to the CHARMM22 parametrization.[33] A few additional runs were also performed on systems containing the partially methylated, 6-mono-*O*-methyl-α-CD. Specific interactions involving the ether groups were modeled using the parameters taken from refs 34 and 35. Potential energy parameters involving the ClO_4^- molecule were taken from the work by Liu et al.,[36] whereas water interactions were modeled using the classical TIP3P model.[37] Long range forces were handled by computing Ewald sums, using a particle mesh procedure.[38,39] Because the systems exhibit a net charge, the presence of a neutralizing background was assumed. The time step was set to 1 fs.

Initial coordinates of the α-CD were obtained from X-ray data.[40] The simulation procedure involved the initial orientation of the CD, such that its largest moment of inertia would coincide with the *z*-axis of the simulation box; an equilibration run of 200 ps followed, during which only the solvent molecules were allowed to move, at temperatures close to $T = 700$ K. From then on, the system was gradually cooled to temperatures close to ambient conditions, by multiple rescalings of the atomic velocities during a time interval of 100 ps. During this period, we released the constraints on the CD sites, with the exception of six spherically symmetric, soft harmonic interactions with restoring force $k \sim 15$ kcal mol^{-1} Å^{-2},[41] acting on each glycosidic oxygen site and centered at the corresponding initial positions. This external potential helped to preserve the initial orientation of the CD, with minor modifications of its overall dynamics. Finally, a water lying in the close vicinity of the upper CD rim was replaced by the ClO_4^- guest (see Figure 1).

III. Results

A. Confinement of ClO_4^-. We will begin our analysis by adopting a simple geometrical order parameter, ξ, that describes the degree of confinement of the ion within the host CD cavity:

$$\xi = Z_{PER} - Z_{CD} \tag{1}$$

In the previous equation, Z_{PER} and Z_{CD} stand for the *z*-coordinates of the centers of mass of the perchlorate molecule and CD, respectively (see also Figure 1). Within this context, a magnitude of interest is given by the Gibbs free energy associated with the order parameter, namely,

$$-\beta G(\tilde{\xi}) \propto \ln \langle \delta(\xi - \tilde{\xi}) \rangle \tag{2}$$

where $\langle ... \rangle$ represents an equilibrium ensemble average and $\beta^{-1} = k_B T$ is the temperature times the Boltzmann constant.

In Figure 2 we present results for $\Delta G(\xi) = G(\xi) - G(\xi{=}\infty)$. Sampling of all relevant fluctuations along different values of ξ was obtained by implementing an adaptive biasing force (ABF) scheme.[42−44] This methodology has been successfully employed in analyses of encapsulation processes involving even more complex guest molecules, such as cholesterol[30] or rotaxane,[31] and relies on the generation of trajectories along a chosen reaction coordinate, experiencing practically no free energy barriers. This is achieved by means of biasing forces estimated along a series of small bins which, in turn, span the complete ξ interval. These forces are applied to flatten the free energy surface, so that ξ becomes uniformly sampled.

Additional technical details of the procedure are summarized as follows: (i) the profile was obtained by dividing the relevant $-10 \lesssim \xi \lesssim 10$ Å interval into 10 different overlapping windows; (ii) a confining potential along the *x* and the *y* directions, with harmonic constant $k_{x-y} \sim 0.1$ kcal mol^{-1} Å^{-2}, was also applied on the ClO_4^- center of mass, which restricted the sampling over the $\rho_{PER}^2 = X_{PER}^2 + Y_{PER}^2 \lesssim 50$ Å^2 cylindrical region, at all values of ξ; (iii) within each window, instantaneous values of the forces were harvested in bins 0.1 Å wide. Convergence within each window typically required a sequence of $\sim 2 \times 10^6$ simulation steps.

The free energy profile for ClO_4^- inclusion shown in Figure 2 (solid line) exhibits a central barrier flanked by two local minima: the deepest one ($\Delta G \sim -2.5$ kcal mol^{-1}) is located near the positions of the O6-HO6 primary hydroxyl groups, $\xi_0 \sim -2.75$ Å (see Figure 1), whereas the second one, somewhat wider and shallower ($\Delta G \sim -0.5$ kcal mol^{-1}) is centered at $\xi \sim 5$ Å, close to the location of the hydroxylated α-CD upper rim. The magnitude of the central barrier, located at $\xi \sim 0$, is $\Delta G \sim 2.5(4.5)$ kcal mol^{-1} high, measured from the right (left) minimum.

Estimates for the standard free energy for the encapsulation ΔG^0_{enc} can be readily obtained from $\Delta G(\xi)$, namely,

$$-\beta \Delta G^0_{enc} = \ln \frac{A \int_{-\infty}^{\infty} \exp[-\beta \Delta G(\xi)]\, d\xi}{dm^3} = 2.5 \tag{3}$$

where $A = 1.6 \times 10^{-16}$ dm^2 represents an estimate of the average section of an α-CD. A comparison between the previous result and direct experimental information is not straightforward: the available results exhibit a widespread dispersion and strongly

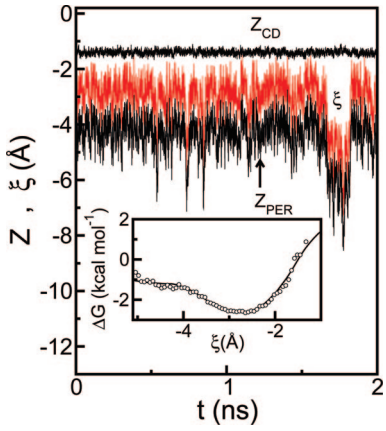

Figure 3. Time evolution of the reaction coordinate, ξ and its two components, Z_{PER} and Z_{CD}. In the inset, we show a comparison between the free energy profile obtained from a histogram of $\xi(t)$ (open circles) and the ABF profile shown in Figure 2 (solid line).

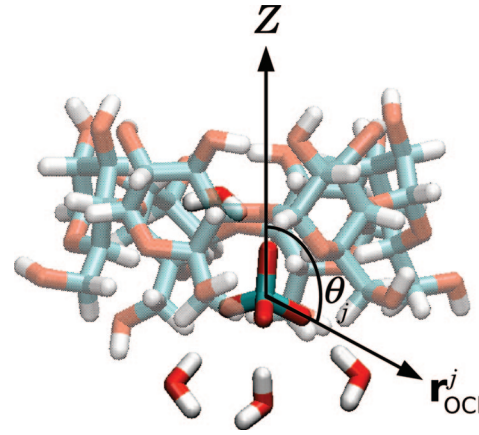

Figure 4. Snapshot of a typical stable configuration for the inclusion of ClO_4^- within an α-CD. Also shown are the four nearest water neighbors of the host and relevant directions which define the angles θ_j (see text).

depend on the particular technique implemented, the ionic strength and the specific counterions presented in solutions. For example, using NMR signals, Yamashoji et al.[7] have reported $-\beta\Delta G^0_{enc} = 2.8$ for $NaClO_4$, whereas pH potentiometric measurements performed by Gelb et al.[12] yield $-\beta\Delta G^0_{enc} \sim 4$, for buffered solutions containing ClO_4^-, to cite two well differentiated experimental results. As such, the 0.3 k_BT discrepancy between our result for ΔG^0_{enc} and Yamashoji's is still smaller than the overall experimental uncertainty (of the order of 1.2 k_BT); this observation leads us to believe that our description may still remain physically sound.

Given this picture, we further investigated on the characteristics of the configurations in the vicinity of the global minimum. To that end, an additional nonbiased simulation experiment was undertaken, with the ClO_4^- initially equilibrated at the vicinity of $\xi_0 \sim -2.75$ Å. Note that the depth of the attractive potential well is sufficient so as to allow us to collect meaningful statistics in this region for time spans of the order of a couple of nanoseconds. In Figure 3 we present results for the time evolution of $\xi(t)$, $Z_{PER}(t)$ and $Z_{CD}(t)$. Except for a brief 150 ps interval at $t \sim 1.8$ ns (corresponding to a frustrated release episode of the guest molecule), $\xi(t)$ fluctuates around $\xi_0 = -2.89 \pm 0.56$ Å. Interestingly, a free energy profile obtained from the logarithm of the probability distribution associated with $\xi(t)$ at the vicinity of ξ_0 (see inset in Figure 3) yields a similar curvature for the global minimum as that presented in Figure 2.

In Figure 4 we present a snapshot of a typical configuration of the solvation structure of a trapped ClO_4^- at the global minimum. At a first glance, the overall structure can be described in terms of a tetracoordinated solute interacting exclusively with water molecules, via hydrogen bonds: one water molecule clearly lies within the CD cavity whereas the other three are located in outer positions, near the lower rim.

To gain quantitative insight about this structure, we analyzed site−site pair correlation functions involving Oxygen sites of ClO_4^- and hydrogen sites of water:

$$g_{OH}(r) = \frac{V}{4\pi r^2 2\, N_w\, 4} \sum_{i=1}^{2N_w} \sum_{j=1}^{4} \langle (\delta |r_i^H - r_j^O| - r) \rangle \quad (4)$$

where r_i^H and r_j^O correspond to coordinates of the ith hdrogen site ($1 \le i \le 2N_w$) in the water molecules and the jth oxygen site ($1 \le j \le 4$) in the ClO_4^-, respectively. Results for the

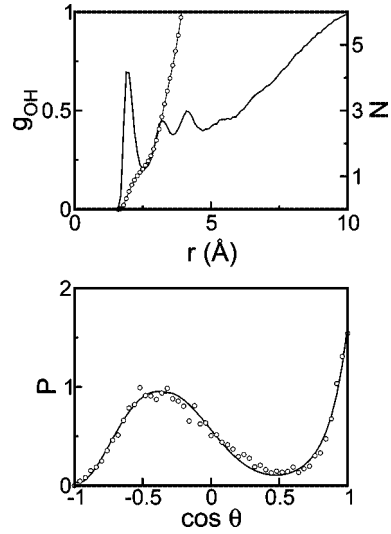

Figure 5. Upper panel: g_{OH} corresponding to ClO_4-H_2O site−site pair correlation function. The cumulative integral, N, is also shown (right axis, open circles). Bottom panel: orientational correlation, $P(\cos\theta)$, for configurations at the vicinity of the free energy minimum.

site−site pair correlation function are shown in the top panel of Figure 5. The profile is dominated by a main peak located at $r = 2$ Å, corresponding to a single, lineal, $O-H_w\cdots O_{PER}$ hydrogen bond (results for the cumulative integral are also shown in Figure 5).

A close inspection of Figure 4 also reveals that one Cl−O bond is distinctively aligned along the z-axis. To quantify this particular orientational correlation, we computed the following distribution:

$$P(\cos\theta) = \frac{1}{4}\sum_{j=1}^{4} \langle \delta(\cos\theta_j - \cos\theta) \rangle \quad (5)$$

with

$$\cos\theta_j = \frac{\mathbf{r}^j_{OCl} \cdot \hat{\mathbf{z}}}{|\mathbf{r}^j_{OCl}|} \quad (6)$$

where $\mathbf{r}^j_{OCl} = \mathbf{r}^j_O - \mathbf{r}_{Cl}$ ($1 \le j \le 4$) and z represents a unit vector along the z-direction (see also Figure 4).

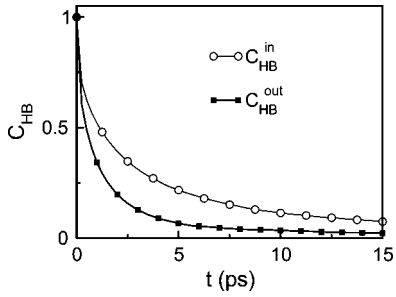

Figure 6. Hydrogen bond survival probability function, $C_{HB}(t)$, for bonds between ClO_4^- and water, computed during the period of time the host molecule remains in the interior of the CD cavity (C_{HB}^{in}, circles). For comparison, the function $C_{HB}^{out}(t)$, corresponding to the ClO_4^- molecule solvated in bulk water, is also shown (squares).

Results for $P(\cos\theta)$ are shown in the bottom panel of Figure 5. A bimodal distribution is clearly perceptible: (i) on the one hand, there is a local maximum, integrating approximately ~0.75, located at $\cos\theta \sim -0.3$, a value quite close to the minimum of the corresponding bending interaction $\theta \sim 109.5°$; (ii) on the other hand, the distribution presents a second peak, well separated from the previous one, at $\cos\theta \sim 1$, with area ~0.25.

To further corroborate the stability of the tetracoordination of the ClO_4^- with the water molecules, we estimated τ_{HB}, the average lifetime of the four tagged solute−solvent hydrogen bonds (HB). To do so, we computed the time integral of the time correlation function of the occupation number η_{ij},

$$\tau_{HB} = \int_0^\infty C_{HB}(t)\,dt \tag{7}$$

$$C_{HB}(t) = \sum_{ij} \frac{\langle \eta_{ij}(t)\,\eta_{ij}(0)\rangle}{\langle \eta_{ij}^2\rangle} \tag{8}$$

where $\eta_{ij}(t) = 1$ if the ClO_4^- (ith molecule in eq 8) is H-bonded to the jth water molecule at time t and zero otherwise, in the intermittent approximation.[45−48] For the definition of HB, we used the geometrical criterion described in ref 49.

To compute τ_{HB}, we split the full temporal interval into two parts: during the first one ("in"), the ClO_4^- remained trapped in the interior of the α-CD cavity, and during the second one ("out"), we sampled configurations with the ClO_4^- solvated in the bulk. Results for $C_{HB}(t)$ corresponding to the two periods are shown in Figure 6. Integrals over the two curves yield $\tau_{HB}^{out} = 2.1$ ps and $\tau_{HB}^{in} = 6$ ps. This enhancement in the HB characteristic time scale, of approximately a factor of 3, would then confirm the extra-stability of the first solvation structure provided by the CD.

B. Confinement of Different ClO_4-like Guests. We now turn into the analysis of the nature of the encapsulation mechanism for small ionic species. In this context we found it instructive to perform two series of runs in which the ClO_4^- guest was replaced by (i) an artificial cation, hereafter referred to as ClO_4^+, obtained by reversing the original partial charges of the anion and (ii) a neutral-like ClO_4 hydrophobic molecule, in which all Coulomb charges were suppressed.

For a direct comparison, the free energy profiles associated with these new species are also displayed in Figure 2. The profile of ΔG for ClO_4^+ is dominated by a ~8.2 kcal mol^{-1} main maximum, located at $\xi = -1.3$ Å. As we move to positive values of ξ, a plateau-like regime appears, localized between 0 $\lesssim \xi \lesssim$ 3 Å, where ΔG briefly levels off at ~3.5 kcal mol^{-1}. Taking into account these observations, one can conclude that no encapsulation processes are likely to be observed for the cationic guests; moreover, and contrasting sharply with the ClO_4^- result, the lower rim of the CD has now turned into the most unfavorable solvation environment. The third curve shown in Figure 2 corresponds to the hydrophobic ClO_4 solute (dashed line). As expected, in the absence of Coulomb interactions, the central, $\xi \sim 0$, region of the cavity becomes a much more stable solvation medium than the polar bulk solvent ($\Delta G(\xi{=}0) \sim -5$ kcal mol^{-1}). As such, our results corroborate previous interpretations based on thermodynamic data analyses[12] that have suggested that Coulomb forces play a leading role controlling the complexation of small ionic species within CD cavities, in detriment of the hydrophobic interactions, which are normally invoked as the ones driving similar encapsulation processes for larger and more complex organic guests.

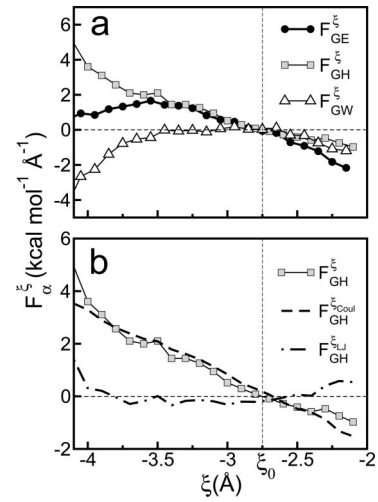

Figure 7. (a) Mean forces acting upon the ClO_4^- molecule at the vicinity of the free energy minimum, ξ_0. Also shown are the contributions from guest−host and guest−water interactions. (b) Decomposition of the guest−host average force into Coulombic and dispersion (Lennard-Jones) contributions.

C. Stability Analysis. To further investigate on the validity of the previous arguments, we examined with more detail the sources of the stabilization of the anionic guests in the vicinity of global minimum of ΔG at $\xi_0 \sim -2.75$ Å. Our analysis was based on the consideration of the total guest-environment energy coupling E_{GE}, namely,

$$E_{GE} = E_{GH} + E_{GW} \tag{9}$$

where E_{GH} and E_{GW} represent the guest−host and guest−water contributions to the total intermolecular potential energy. Note that an equivalent partition can also be performed in terms of average forces along the ξ direction, namely,

$$F_{GE}^{\xi} = F_{GH}^{\xi} + F_{GW}^{\xi} \tag{10}$$

$$F_{\alpha}^{\xi} = -\left\langle \frac{\partial E_{\alpha}}{\partial \xi} \right\rangle$$

with α = GH, GW. The results for the average force and its guest−host and guest−water decomposition as a function of the order parameter are shown in the top panel of Figure 7. The results were collected over the ~2 ns unconstrained

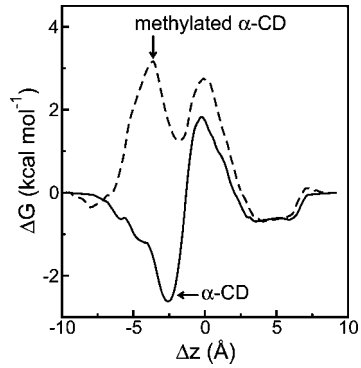

Figure 8. Free energy profiles for the inclusion of ClO_4^- into a normal and a methylated α-CD.

trajectory mentioned in previous sections. The interval sampled is rather narrow, spanning from $\xi \sim -4$ Å, which roughly corresponds to the location of the lower rim, up to $\xi \sim -2$ Å, which is still slightly below the position of the center of mass of the CD. Note that interactions with the solvent, except for the $\xi \lesssim -3.5$ Å interval where the water "pushes" the guest out toward the bulk, practically vanish inside the inner cavity of the CD. Anyhow, the magnitude of the solvent forces is much smaller than those derived from the interactions with the CD, that clearly dominate the stabilization of the guest−host complex. Moreover, a second decomposition of the latter force into dispersive, i.e., Lennard-Jones type, and Coulombic contributions (shown in the bottom panel of Figure 7) reveals that Coulomb interactions prevail in promoting the stabilization of the ClO_4^- within CD cavities.

Looking for additional elements supporting our description, we finally constructed the free energy profile corresponding to the encapsulation of ClO_4^- within the partially methylated, 6-mono-*O*-methyl-α-CD. This functionalization enhances the hydrophobicity of the CD central cavity and also leads to a small increase of the linear dimensions of the molecule along the z axis. The profile for the corresponding free energy is presented in Figure 8; note that to minimize effects deriving from the larger size of the cavity, the curves in Figure 8 are depicted as a function of $\Delta z = Z_{PER} - \bar{Z}$, where $\bar{Z}$ represents the average z-coordinate of the six glycosidic oxygen sites in the cyclodextrins. As expected, the new profile exhibits dramatic changes in the negative Δz region: (i) the most remarkable is observed in the vicinity of the formerly stable solvation environment, that now turns into a highly unfavorable region, characterized by a $\Delta G \sim 3$ kcal mol^{-1} high barrier. (ii) The position of the new minimum is shifted ≈1 Å toward the central part of the cavity; from this point, the magnitude of the escape activation energy in either direction is not negligible ∼2 kcal mol^{-1} ∼ 4 k_BT. The operated functionalization does not promote any meaningful modification in the profile along the $\Delta z \gtrsim 0$ region, in which the partial stabilization is still dominated by interactions with the hydroxyl groups of the upper rim.

IV. Concluding Remarks

The simulation results presented in this paper provide new insights concerning the nature of the encapsulation of ClO_4^- within the hydrophobic cavity of an α-CD. Using an ABF scheme, we succeeded in constructing a free energy profile associated to a simple geometrical order parameter that describes the degree of encapsulation. The profile presents a global minimum located at the vicinity of the primary hydroxyl groups and a much shallower one, at the upper rim. On the other hand, this feature is in agreement with previous interpretations inferred from experimental results.[8,9] The central part of the CD cavity represents a highly unfavorable environment for ionic trapping. By means of a simple integration of the free energy profile along the relevant portion of the phase space, we also obtained an estimate for the Gibbs free energy associated to the binding. Our result is somewhat higher (∼0.3 kcal mol^{-1} less stable) than the ones reported in previous experimental studies. Anyhow, the discrepancy may be ascribed to differences between our simplified simulated system and the ones actually measured, most notably, those associated with the presence of counterions and/or additional ionic species. In this context, we would like to stress that experimental information confirms that cations are hardly incorporated within CD cavities[50] (a fact that was furthermore confirmed in our simulations with ClO_4^+). As such, we tend to believe that their presence in the analysis of the complexation of ClO_4^- can be safely disregarded.

From a microscopic perspective, the stable encapsulation configurations of ClO_4^- are characterized by the tetracoordination with neighboring water molecules via hydrogen bonds. This intermolecular connectivity, in turn, also affects orientational correlations of the guest ion that presents one Cl−O bond aligned along the axis of the cylindrical cavity of the CD.

Changes in the charge distribution of the solute modify the corresponding free energy profiles. For a ClO_4^+-like ion, we found that the inner cavity does not exhibit any stable environment for encapsulation. The scenario changes dramatically as the solute turns into an hydrophobic species: under these circumstances, the free energy profile at the central segment of the α-CD cavity shows a minimum, whose depth is at least 1 order of magnitude larger than typical thermal energies.

Finally, we also analyzed ionic trapping within a partially functionalized CD, in which the primary hydroxyl groups are methylated. Our results clearly show the disappearance of the main minimum, revealing that the highly polarized OH groups control the encapsulation mechanism of the anion. As stated in the previous paragraph, these CD groups do not lie within the first solvation shell of the ClO_4^-. This observation, in turn, would indicate that the stability of the anion solvation structure provided by OH groups is somehow exerted in an indirect fashion, most likely affecting not only the individual ion but also its first solvation shell. Although this feature has been conjectured in the past,[8,50] the results presented here provide, for the first time, direct confirmation of the complexity in the solvation of ionic species within CD cavities. We are confident that the physical arguments supporting this evidence will remain valid in the analysis of the solvation of other small ionic solutes that we are currently undertaking.

Acknowledgment. We thank Professor Daniel Laria for many illuminating discussions and valuable suggestions, and for thoroughly reading this manuscript. J.R. and M.D.E. are members of Carrera de Investigador Científico de CONICET (Argentina).

References and Notes

(1) Connors, K. A. *Chem. Rev.* **1997**, *97*, 1325.
(2) For comprehensive information about cyclodextrins, see the special issue: *Chem. Rev.* **1998**, *98*.
(3) Recently, cyclodextrins composed of as many as 40−50 units have been reported. See, for example: Ivanov, P. M.; Jaime, C. *J. Phys. Chem. B* **2004**, *108*, 6261.
(4) Wojcik, J. F.; Rohrbach, R. P. *J. Phys. Chem.* **1975**, *79*, 2251.
(5) Rohrbach, R. P.; Rodriguez, L. J.; Eyring, E. M.; Wojcik, J. F. *J. Phys. Chem.* **1977**, *81*, 944.
(6) Buvari, A.; Barcza, L. *J. Incl. Phenom.* **1989**, *7*, 379.

(7) Yamashoji, Y.; Fujiwara, M.; Matsushita, T.; Tanaka, M. *Chem. Lett.* **1993**, *22*, 1029.
(8) Matsui, Y.; Ono, M.; Tokunaga, S. *Bull. Chem. Soc. Jpn.* **1997**, *70*, 535.
(9) McMullan, R. K.; Saenger, W.; Fayos, J.; Mootz, D. *Carbohydr. Res.* **1973**, *31*, 37.
(10) Godínez, L. A.; Patel, S.; Criss, C. M.; Kaifer, A. E. *J. Phys. Chem.* **1995**, *99*, 17449.
(11) Rekharsky, M. V.; Inoue, Y. *J. Am. Chem. Soc.* **2002**, *124*, 813.
(12) Gelb, R. I.; Schwartz, L. M.; Radeos, M.; Laufer, D. A. *J. Phys. Chem.* **1983**, *87*, 3349.
(13) Lewis, E. A.; Hansen, L. D. *J. Chem. Soc., Perkin Trans.* **1973**, *2*, 2081.
(14) Spencer, J. N.; He, Q.; Ke, X.; Wu, Z.; Fetter, E. *J. Solution Chem.* **1998**, *27*, 1009.
(15) Lipkowitz, K. *Chem. Rev* **1998**, *98*, 1829. For example, see the entries in Tables 2 and 3, where a large body of molecular dynamics studies involving different CD-guest partners are reported.
(16) Caballero, J.; Zamora, C.; Aguayo, D.; Yanez, C.; Gonzalez-Nilo, F. D. *J. Phys. Chem. B* **2008**, *112*, 10194.
(17) Rodriguez, J.; Martí, J.; Guàrdia, E.; Laria, D. *J. Phys. Chem. B* **2008**, *112*, 8990.
(18) Raffaini, G.; Ganazzoli, F. *J. Incl. Phenom.* **2007**, *57*, 683.
(19) Georg, H. C.; Coutinho, K.; Canuto, S. *Chem. Phys. Lett.* **2005**, *413*, 16.
(20) Choi, Y.; Jung, S. *Carbohydr. Res.* **2004**, *339*, 1961.
(21) Franchi, P.; Lucarini, M.; Mezzina, E.; Pedulli, G. F. *J. Am. Chem. Soc.* **2004**, *126*, 4343.
(22) Shilov, I. Y.; Kurnikova, M. G. *J. Phys. Chem. B* **2003**, *107*, 7189.
(23) Mele, A.; Raffaini, G.; Ganazzoli, F.; Juza, M.; Schurig, V. *Carbohydr. Res.* **2003**, *338*, 625.
(24) Bonnet, P.; Jaime, C.; Morin-Allory, L. *J. Org. Chem.* **2002**, *67*, 8602.
(25) Guernelli, S.; Lagana, M. F.; Spinelli, D.; Lo Meo, P.; Noto, R.; Riela, S. *J. Org. Chem.* **2002**, *67*, 2948.
(26) Oana, M.; Tintaru, A.; Gavriliu, D.; Maior, O.; Hillebrand, M. *J. Phys. Chem. B* **2002**, *106*, 257.
(27) Mu, T. W.; Liu, L.; Li, X. S.; Guo, Q. X. *J. Phys. Org. Chem.* **2001**, *14*, 559.
(28) Bonnet, P.; Jaime, C.; Morin-Allory, L. *J. Org. Chem.* **2001**, *66*, 689.
(29) Salvatierra, D.; Sanchez-Ruiz, X.; Garduno, R.; Cervello, E.; Jaime, C.; Virgili, A.; Sanchez-Ferrando, F. *Tetrahedron* **2000**, *56*, 3035.
(30) Yu, Y.; Chipot, C.; Cai, W.; Shao, X. *J. Phys. Chem. B* **2006**, *110*, 6372.
(31) Yu, Y.; Chipot, C.; Sun, T.; Shao, X. *J. Phys. Chem. B* **2008**, *112*, 5268.
(32) Phillips, J. C.; Braun, R.; Wang, W.; Gumbart, J.; Tajkhorshid, E.; Villa, E.; Chipot, C.; Skeel, R. D.; Kale, L.; Schulten, K. *J. Comput. Chem.* **2005**, *26*, 1781.
(33) MacKerell, J.A. D.; Bashford, D.; Bellott, M.; Dunbrack, J. R. L.; Evanseck, J. D.; Field, M. J.; Fischer, S.; Gao, J.; Guo, H.; Ha, S.; Joseph-McCarthy, D.; Kuchnir, L.; Kuczera, K.; Lau, F. T. K.; Mattos, C.; Michnick, S.; Ngo, T.; Nguyen, D. T.; Prodhom, B.; W. E.; Reiher, I. W. E.; Roux, B.; Schlenkrich, M.; Smith, J. C.; Stote, R.; Straub, J.; Watanabe, M.; Wiórkiewicz-Kuczera, J.; Yin, D.; Karplus, M. *J. Phys. Chem. B* **1998**, *102*, 3586.
(34) Vorobyov, I.; Anisimov, V. M.; Greene, S.; Venable, R. M.; Moser, A.; Pastor, R. W.; MacKerell, A. D., Jr. *J. Chem. Theory Comput.* **2007**, *3*, 1120.
(35) Lee, H.; Venable, R. M.; MacKerell, A. D., Jr.; Pastor, R. W. *Biophys. J.* **2008**, *95*, 1590.
(36) Liu, X.; Zhang, S.; Zhou, G.; Wu, G.; Yuan, X.; Yao, X. *J. Phys. Chem. B* **2006**, *110*, 12062.
(37) Jorgensen, W. L.; Chandrasekhar, J.; Madura, J.; Impey, R. W.; Klein, M. L. *J. Chem. Phys.* **1983**, *79*, 926.
(38) Darden, T. A.; York, D. M.; Pedersen, L. G. *J. Chem. Phys.* **1993**, *98*, 10089.
(39) Essmann, U.; Perera, L.; Berkowitz, M. L.; Darden, T.; Lee, H.; Pedersen, L. G. *J. Chem. Phys.* **1995**, *103*, 8577.
(40) Available at http://xray.bmc.uu.se/hicup//ACX/index.html, Hetero - compound Information Centre - Uppsala.
(41) Hwang, H.; Schatz, G. C.; Ratner, M. A. *J. Phys. Chem. B* **2006**, *110*, 26448.
(42) Darve, E.; Pohorille, A. *J. Chem. Phys.* **2001**, *115*, 9169.
(43) Hénin, J.; Chipot, C. *J. Chem. Phys.* **2004**, *121*, 2904.
(44) Rodriguez-Gomez, D.; Darve, E.; Pohorille, A. *J. Chem. Phys.* **2004**, *120*, 3563.
(45) Martí, J.; Padró, J. A.; Guàrdia, E. *J. Chem. Phys.* **1996**, *105*, 639.
(46) Luzar, A. *J. Chem. Phys.* **2000**, *113*, 10663.
(47) Elola, M. D.; Ladanyi, B. M. *J. Chem. Phys.* **2006**, *125*, 184506.
(48) Guàrdia, E.; Laria, D.; Martí, J. *J. Phys. Chem. B* **2006**, *110*, 6332.
(49) Sonoda, M. T.; Skaf, M. S. *J. Phys. Chem. B* **2007**, *111*, 11948.
(50) Høiland, H.; Hald, L. H.; Kvammen, O. J. *J. Solution Chem.* **1981**, *10*, 775.

JP808947M